Host nutrient milieu drives an essential role for aspartate biosynthesis during invasive *Staphylococcus aureus* infection

Aimee D. Potter[a], Casey E. Butrico[a], Caleb A. Ford[b], Jacob M. Curry[c], Irina A. Trenary[d], Srivarun S. Tummarakota[a], Andrew S. Hendrix[c,1], Jamey D. Young[d,e], and James E. Cassat[a,b,c,f,g,2]

[a]Department of Pathology, Microbiology, and Immunology, Vanderbilt University Medical Center, Nashville, TN 37232; [b]Department of Biomedical Engineering, Vanderbilt University, Nashville, TN 37235; [c]Division of Pediatric Infectious Diseases, Department of Pediatrics, Vanderbilt University Medical Center, Nashville, TN 37232; [d]Department of Chemical and Biomolecular Engineering, Vanderbilt University, Nashville, TN 37235; [e]Department of Molecular Physiology and Biophysics, Vanderbilt University, Nashville, TN 37232; [f]Vanderbilt Institute for Infection, Immunology, and Inflammation (VI4), Vanderbilt University Medical Center, Nashville, TN 37232; and [g]Vanderbilt Center for Bone Biology, Vanderbilt University Medical Center, Nashville, TN 37232

Edited by Alice Prince, Columbia University Medical Center, New York, NY, and accepted by Editorial Board Member Carl F. Nathan April 10, 2020 (received for review December 18, 2019)

The bacterial pathogen *Staphylococcus aureus* is capable of infecting a broad spectrum of host tissues, in part due to flexibility of metabolic programs. *S. aureus*, like all organisms, requires essential biosynthetic intermediates to synthesize macromolecules. We therefore sought to determine the metabolic pathways contributing to synthesis of essential precursors during invasive *S. aureus* infection. We focused specifically on staphylococcal infection of bone, one of the most common sites of invasive *S. aureus* infection and a unique environment characterized by dynamic substrate accessibility, infection-induced hypoxia, and a metabolic profile skewed toward aerobic glycolysis. Using a murine model of osteomyelitis, we examined survival of *S. aureus* mutants deficient in central metabolic pathways, including glycolysis, gluconeogenesis, the tricarboxylic acid (TCA) cycle, and amino acid synthesis/catabolism. Despite the high glycolytic demand of skeletal cells, we discovered that *S. aureus* requires glycolysis for survival in bone. Furthermore, the TCA cycle is dispensable for survival during osteomyelitis, and *S. aureus* instead has a critical need for anaplerosis. Bacterial synthesis of aspartate in particular is absolutely essential for staphylococcal survival in bone, despite the presence of an aspartate transporter, which we identified as GltT and confirmed biochemically. This dependence on endogenous aspartate synthesis derives from the presence of excess glutamate in infected tissue, which inhibits aspartate acquisition by *S. aureus*. Together, these data elucidate the metabolic pathways required for staphylococcal infection within bone and demonstrate that the host nutrient milieu can determine essentiality of bacterial nutrient biosynthesis pathways despite the presence of dedicated transporters.

metabolism | pathogenesis | *Staphylococcus aureus* | osteomyelitis | aspartate

Staphylococcus aureus is a gram-positive human pathogen that causes life-threatening, invasive disease, imposing a significant healthcare burden in the United States and globally (1). *S. aureus* is known to colonize nearly every human tissue. The ability of *S. aureus* to survive in unique host environments relates directly to its ability to obtain essential nutrients from host tissues (2, 3). It is therefore vital to understand how pathogens obtain nutrients in the context of invasive infection and inflammatory-associated shifts in the host nutrient milieu.

As one of the most common manifestations of invasive *S. aureus* infection, osteomyelitis (OM) is a paradigm for invasive staphylococcal disease (4). Bone infections cause significant morbidity, including bone damage, pathologic fractures, and septicemia, even in the presence of appropriate treatment (5, 6). The bone destruction observed during infection suggests that *S. aureus* experiences a dynamic nutrient environment inside the host, as host consumption and release of nutrients are altered by widespread cell death and inflammation. Furthermore, although normal skeletal remodeling occurs at homeostasis, invading pathogens alter the kinetics of bone remodeling, in part via changes in skeletal cell differentiation and activation (7, 8). This bone remodeling is coordinated by the opposing action of bone-resorbing osteoclasts and bone-depositing osteoblasts—both of which exhibit a highly glycolytic metabolism (9–12). The dynamic nature of bone during infection consequently makes OM a unique model for the study of fundamental processes in bacterial nutrient acquisition and metabolism.

In order to elucidate the genetic pathways required by staphylococci during infection, we previously conducted transposon sequencing (TnSeq) analysis in an *S. aureus* murine OM model (13). TnSeq revealed that a majority of the genes required for staphylococcal survival during OM are in metabolic pathways. However, the use of TnSeq to examine bacterial metabolism is confounded by both exchange and competition for metabolites

Significance

***Staphylococcus aureus* can infect a diverse array of host environments. The broad tissue tropism of *S. aureus* requires metabolic flexibility to utilize the variety of nutrient sources found within target organ systems. In this work, we conducted a systematic analysis of the central metabolic pathways required for *S. aureus* survival during bone infection, one of the most frequent sites of invasive staphylococcal disease. We show that *S. aureus* requires aspartate biosynthesis to survive during bone infection, despite possessing an aspartate transporter, due to inhibition of aspartate utilization by the amino acid glutamate. Our results reveal a crucial role for inflammation-associated shifts in the host nutrient milieu for determining the metabolic pathways utilized by *S. aureus* during invasive infection.**

Author contributions: A.D.P., J.D.Y., and J.E.C. designed research; A.D.P., C.E.B., C.A.F., J.M.C., I.A.T., A.S.H., and J.E.C. performed research; I.A.T. processed samples for GCMS; A.D.P., C.E.B., J.M.C., and S.S.T. contributed new reagents/analytic tools; A.D.P., J.D.Y., and J.E.C. analyzed data; and A.D.P. and J.E.C. wrote the paper.

The authors declare no competing interest.

This article is a PNAS Direct Submission. A.P. is a guest editor invited by the Editorial Board.

[1]Present address: College of Medicine and Life Sciences, The University of Toledo, Toledo, OH 43606.

[2]To whom correspondence may be addressed. Email: jim.cassat@vumc.org.

This article contains supporting information online at https://www.pnas.org/lookup/suppl/doi:10.1073/pnas.1922211117/-/DCSupplemental.

First published May 15, 2020.

between mutants, which may mask or exacerbate phenotypes in vivo (14). Additionally, the generation of an *S. aureus* transposon library in rich media introduces a significant selection bias against mutants in glycolysis. This bias in library generation inhibits comprehensive analysis of the metabolic pathways required for survival during infection. Therefore, to better understand the metabolic pathways that allow *S. aureus* to survive within the host nutritional milieu, we sought to comprehensively assess the central metabolic pathways required for staphylococcal survival in bone.

Results

***S. aureus* Requires Glycolysis but Not Gluconeogenesis during OM.** In order to synthesize essential cellular macromolecules, *S. aureus* requires 12 essential biosynthetic intermediates (Fig. 1) (2). Six of these essential intermediates are produced by glycolysis and gluconeogenesis. Because skeletal cells exhibit a highly glycolytic metabolism, we hypothesized that competition with the host for available glucose during OM would necessitate the use of alternative nutrient sources, such as amino acids, to produce the biosynthetic precursors generated from glycolysis/gluconeogenesis. We therefore hypothesized that gluconeogenesis would be essential for *S. aureus* survival during OM. This hypothesis is supported by the fact that *pyc*, encoding the enzyme pyruvate carboxylase which feeds precursors into gluconeogenesis by converting pyruvate into oxaloacetate, was identified as essential for *S. aureus* survival in bone by TnSeq (Fig. 1) (13). However, Pyc also contributes to several additional metabolic pathways, including the tricarboxylic acid (TCA) cycle and amino acid synthesis (Fig. 1). Therefore, to test the role of gluconeogenesis in *S. aureus* pathogenesis during OM, we examined the survival of mutants in both *pyc* and *pckA*. PckA is a dedicated gluconeogenic enzyme that catalyzes the conversion of the metabolic product of Pyc, oxaloacetate, into phosphoenolpyruvate (Fig. 1). We found that disruption of *pyc* had a significant effect on the fitness of *S. aureus* during OM (Fig. 2). Surprisingly, however, *pckA* was not essential for survival, indicating that gluconeogenesis is not required for staphylococcal survival during OM. Due to the absence of a survival defect in a gluconeogenic mutant in vivo, we postulated that glycolytic carbon sources may in fact be readily available to *S. aureus* in vivo to fuel bacterial glycolysis. To test this hypothesis, we examined the in vivo survival of mutants in *pyk*, which encodes the glycolytic enzyme responsible for synthesizing pyruvate from phosphoenolpyruvate. We found that *S. aureus* requires *pyk* to survive in bone, indicating that glycolysis is indeed required to fuel *S. aureus* growth in vivo during OM (Fig. 2). To further examine the role of glycolysis during OM and to determine if the glycolytic dependence of *S. aureus* in bone was strain-dependent, we also tested the survival of mutants in *pyk* and *pfkA* (encoding the glycolytic enzyme phosphofructokinase) in the Newman-strain background (*SI Appendix*, Fig. S1). Despite the increased bacterial burdens of the Newman strain in our OM model, inactivation of both *pyk* and *pfkA* resulted in significant fitness defects compared with the wild type (WT) during OM, consistent with results using USA300-lineage mutants. Together, these results show that glycolysis, not gluconeogenesis, provides essential biosynthetic intermediates for *S. aureus* during infection of bone.

The Pentose Phosphate Pathway Enzyme TalA and the TCA Cycle Are Dispensable for Survival during OM. Three essential biosynthetic intermediates can be produced using the pentose phosphate pathway (Fig. 1). Because only one of the enzymes in this pathway is not essential for growth in vitro, we could only test the transaldolase (*talA*) mutant for survival in vivo. A *talA* mutant did not have a survival defect during OM (Fig. 2). Because TalA is redundant or dispensable in several other organisms, we cannot form a conclusion on the unique essentiality of the pentose phosphate pathway as a whole during OM from this experiment (2, 15).

The final three essential biosynthetic precursors for *S. aureus* growth consist of the TCA-cycle intermediates alpha-ketoglutarate (α-KG) and oxaloacetate, and acetyl-coenzyme A (acetyl-CoA), which serves as a link between glycolysis and the TCA cycle. *S. aureus* must therefore utilize either the TCA cycle or metabolite-replenishing reactions, known as anaplerotic reactions, for growth. To determine the role of TCA-cycle enzymes during OM, we examined the survival of mutants in acetyl-CoA synthesis and in each step of the TCA cycle in vivo (Fig. 2). Although a *pdhA* mutant had significantly reduced bacterial burdens in vivo, none of the TCA-cycle mutants tested had defects for survival. Interestingly, a *pdhA* mutant was not as attenuated as the glycolysis mutant *pyk*, likely reflecting the ability of *S. aureus* to still successfully convert pyruvate into oxaloacetate in this mutant background. Instead, the survival defect of a *pdhA* mutant may be reflective of its role as a key enzyme in the utilization of acetyl-CoA in other downstream metabolic pathways such as fatty acid synthesis (Fig. 1). However, overall, these data indicate that the TCA cycle is not essential for survival during OM and that the dependence upon *pdhA* is not driven by a requirement for the TCA cycle.

The Anaplerotic Enzyme AspA Is Required for Bacterial Survival In Vivo. Because the TCA cycle is not required for full bacterial burdens during OM, we hypothesized that the remaining essential biosynthetic intermediates, α-KG and oxaloacetate, would be produced through anaplerotic reactions (Fig. 1). To test this hypothesis, we examined the survival of mutants in glutamate dehydrogenase (*gudB*), which converts glutamate (Glu) to α-KG, and aspartate aminotransferase (*aspA*), which interconverts aspartate (Asp) and α-KG into oxaloacetate and Glu, respectively (Fig. 2). Interestingly, a *gudB* mutant had no survival defect, suggesting that α-KG may be fulfilled by other reactions in vivo. We next examined the fitness of an *aspA* mutant in vivo and found that it was completely attenuated for growth in bone but could be rescued by complementation in cis (Fig. 2 and *SI Appendix*, Fig. S2). An *aspA* mutant also experienced a survival defect as early as 1 d postinfection and, in several mice, was completely cleared by 7 d (*SI Appendix*, Fig. S3*A*). This phenotype was not unique to bone, as an *aspA* mutant also experienced a survival defect in multiple tissue types following disseminated infection (*SI Appendix*, Fig. S3 *B–D*). Interestingly, AspA resides in a pathway with two additional essential enzymes, Pyc and Pyk, for the synthesis of Asp from glycolytic intermediates, suggesting that Asp biosynthesis serves as a fundamental metabolic strategy for *S. aureus* survival in vivo.

An Ex Vivo Approach for Analyzing the Capacity of *S. aureus* to Acquire Nutrients from Bone. We identified endogenous synthesis of Asp as essential for staphylococcal survival in vivo during OM. To generate a more complete picture of the potential nutrients available for *S. aureus* when growing in bone, we next examined exogenous nutrient acquisition. To do this, we developed an in vitro culture system in which *S. aureus* is grown in chemically defined media with glucose (CDMG) supplemented with homogenized bone. In this culture system, we examined the growth of *S. aureus* metabolic mutants in media depleted of, or replete for, various nutrients. We first assessed the ability of homogenized bone to chemically complement known *S. aureus* auxotrophies (Fig. 3) (16). Surprisingly, homogenized bone was able to increase the growth of *S. aureus* in CDMG lacking every amino acid and nucleotide individually. These data suggest that healthy bone serves as a source of critical nutrients for *S. aureus*.

Considering that the amino acids within homogenized bone could supplement WT *S. aureus* auxotrophies, we expected that in the absence of de novo Asp biosynthesis, *S. aureus* would also

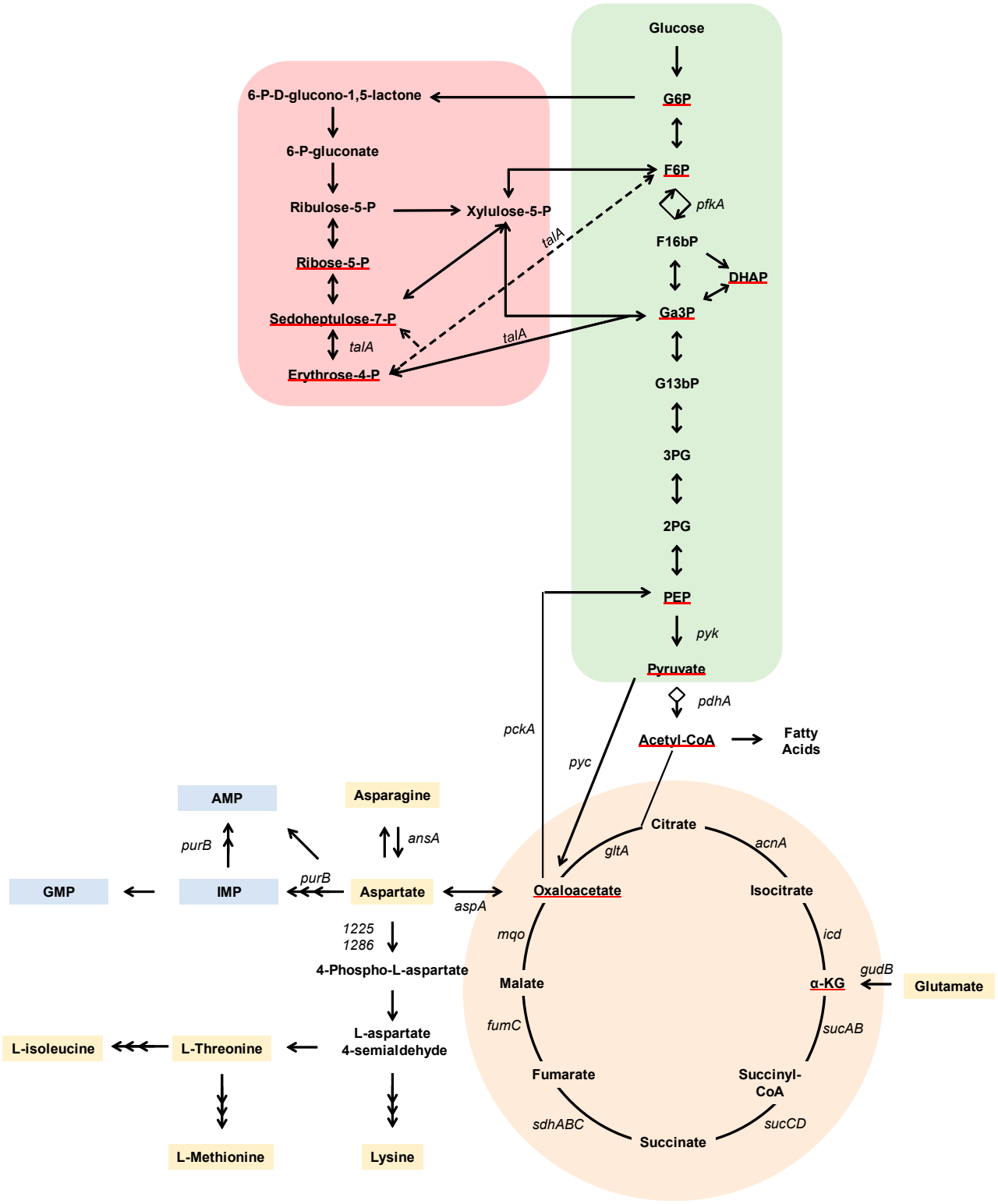

Fig. 1. Schematic of *S. aureus* central metabolism. Metabolites are indicated in bold. Red underline indicates the 12 essential biosynthetic precursors predicted for *S. aureus*. Genes of interest are notated in italics. Green shading indicates glycolysis/gluconeogenesis. Red shading indicates the pentose phosphate pathway. Orange shading indicates the TCA cycle. Yellow shading indicates amino acids. Blue shading indicates purine biosynthesis. AspA and GudB mediate anaplerotic reactions. Multiple arrowheads denote simplification of a multistep pathway. AMP, adenosine monophosphate; DHAP, dihydroxyacetone; F16bP, fructose 1,6-bisphosphate; F6P, fructose-6-phosphate; G13bP, 1,3-bisphosphoglycerate; G2P, 2-phosphoglycerate; G3P, 3-phosphoglycerate; G6P, glucose-6-phosphate; Ga3P, glyceraldehyde 3-phosphate; GMP, guanosine monophosphate; IMP, inosine monophosphate; PEP, phosphoenolpyruvate.

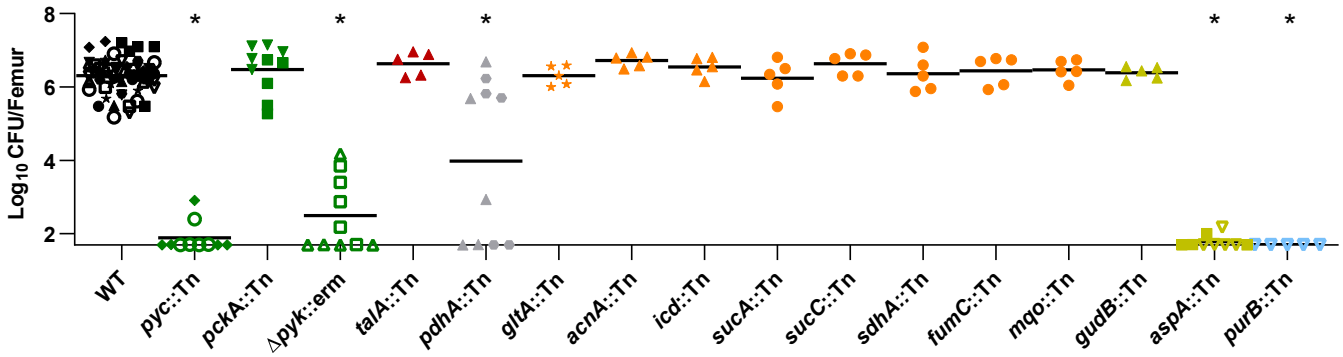

Fig. 2. Central metabolic pathways required for *S. aureus* survival in vivo during osteomyelitis. OM was induced in groups of mice using the indicated strains. At 14 d postinfection, femurs were processed for CFU enumeration. Colored symbols indicate pathways (green, glycolysis/gluconeogenesis enzymes; red, pentose phosphate pathway; orange, TCA cycle; gray, acetyl-CoA synthesis; yellow, anaplerotic reactions; blue, purine biosynthesis). Different shapes indicate independent experiments. Horizontal lines indicate the mean. Statistical significance was determined by Student's *t* test compared with the corresponding WT comparator. Significance of WT vs. *pdhA*::Tn was determined by Mann–Whitney *U* test for bimodal distributions. *$P < 0.05$.

be capable of utilizing exogenous Asp. We therefore hypothesized that an *aspA* mutant may be unable to survive in vivo due to a lack of available exogenous Asp during infection. Because WT *S. aureus* is prototrophic for Asp, an *aspA* mutant was tested to examine the bioavailability of Asp in homogenized bone. An *aspA* mutant was capable of growing to WT levels in CDMG containing exogenous Asp and, as expected, an *aspA* mutant demonstrated an induced auxotrophy for Asp in vitro (Fig. 3). Previous studies have suggested that the requirement for Asp biosynthesis arises from the demand for Asp-derived amino acids, particularly lysine (Lys), in *S. aureus* (17). In keeping with this hypothesis, we found that an *aspA* mutant also demonstrated significantly reduced growth in the absence of Lys, Glu, and purines relative to WT in vitro (Fig. 3). Interestingly, however, homogenized bone could restore growth of an *aspA* mutant when Lys and Glu were individually removed from the medium, suggesting that bone might contain sufficient levels of exogenous Lys and Glu to support *S. aureus* growth. In support of this observation, inactivation of the two aspartate kinase isoforms required for Lys synthesis, *SAUSA300_1225* (*1225*) and *SAUSA300_1286* (*lysC*), reduced *S. aureus* growth in vitro in the absence of Asp-derived amino acids but did not decrease *S. aureus* survival in vivo (*SI Appendix*, Fig. S4). Therefore, Asp-derived amino acids are likely not limiting in bone. On the other hand, homogenized bone could not rescue growth of an *aspA* mutant to WT levels in the absence of Asp or purines, suggesting that these nutrients might be limiting in vivo, or that *S. aureus* is incapable of acquiring Asp or purines from bone (Fig. 3). Taken together, these data indicate that although *S. aureus* is capable of importing Asp and Asp-derived metabolites, bone may not provide sufficient Asp or purines to supplement the growth requirements of *S. aureus* ex vivo, necessitating Asp biosynthesis through AspA.

Deficiency in Purine Biosynthesis Drives the Defect of an *aspA* Mutant In Vivo. Ex vivo assays indicated that, although WT *S. aureus* is prototrophic for purines, the *aspA* mutant developed a purine auxotrophy that could not be rescued by homogenized bone (Fig. 3 and *SI Appendix*, Fig. S5). Asp has multiple roles in purine biosynthesis, and we previously noted that several purine biosynthesis mutants were defective for survival during TnSeq of OM (13). We therefore hypothesized that the survival defect of an *aspA* mutant may be due to an inability to synthesize sufficient purines in vivo. To test if purine biosynthesis is essential for *S. aureus* survival in vivo, we examined survival of a mutant in *purB*, encoding an enzyme that utilizes intermediates derived from Asp to ultimately generate ATP and GTP. We found that disruption of *purB* had a profound effect on the fitness of *S. aureus* (Fig. 2). The essentiality of *purB* indicates that compromising the GTP and ATP branches of purine biosynthesis critically inhibits the ability of *S. aureus* to survive in bone and may drive the survival defect of an *aspA* mutant in vivo. To further evaluate the fate of intracellular Asp in *S. aureus*, we examined the uptake and

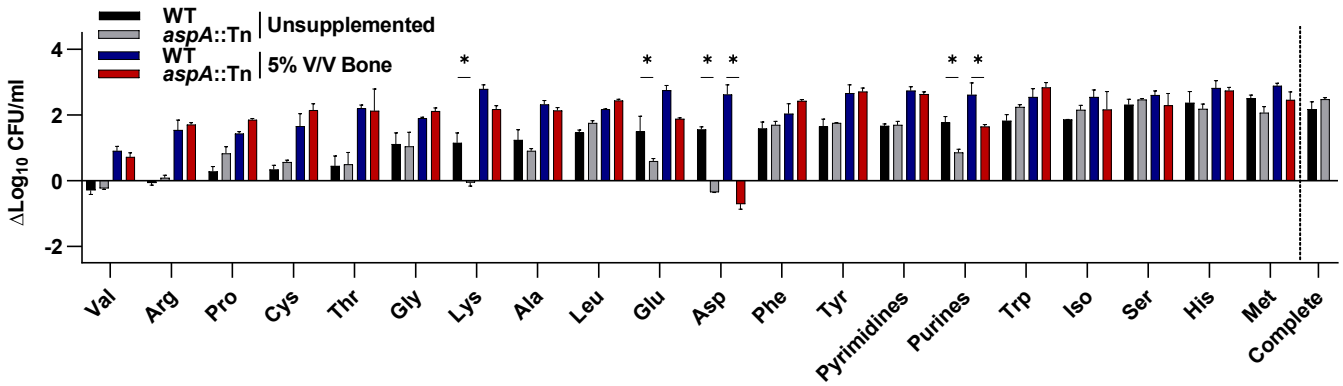

Fig. 3. Bone can supply nutrients required for *S. aureus* growth in vitro. WT or *aspA*::Tn *S. aureus* were grown for 8 h in CDMG lacking the indicated nutrient. Murine femurs were homogenized and added to CDMG lacking the indicated nutrient at 5% V/V. Growth in complete CDMG without bone is shown (*Far Right*). Columns indicate the mean. Error bars represent SEM; $n = 2$ biologic replicates. Significance was determined by two-way ANOVA with Holm–Sidak correction for multiple comparisons for unsupplemented or for the 5% bone condition. *$P < 0.1$.

metabolism of $^{13}C/^{15}N$-labeled Asp by gas chromatography mass spectrometry (GCMS) (Fig. 4 and Dataset S1). Tracking of carbon and nitrogen derived from [$^{13}C_4$,^{15}N]Asp in WT *S. aureus* indicated that Asp-derived heavy atoms are readily incorporated into Glu, citrate, α-KG, and fumarate. In an *aspA* mutant, however, synthesis of Glu, citrate, and α-KG from Asp is almost completely abrogated. Despite the lack of Asp-derived TCA intermediates, an *aspA* mutant is still viable in the presence of exogenous Asp, suggesting that Asp synthesis is essential for alternative metabolic pathways. Instead, in an *aspA* mutant, Asp-derived carbon is converted primarily into M4 fumarate, that is, containing four heavy atoms, which is generated from purine biosynthesis in a pathway reliant upon PurB (Fig. 4). Taken together, these in vivo and GCMS data suggest that an *aspA* mutant relies upon exogenous Asp for purine biosynthesis, which is essential for staphylococcal survival in vivo during OM.

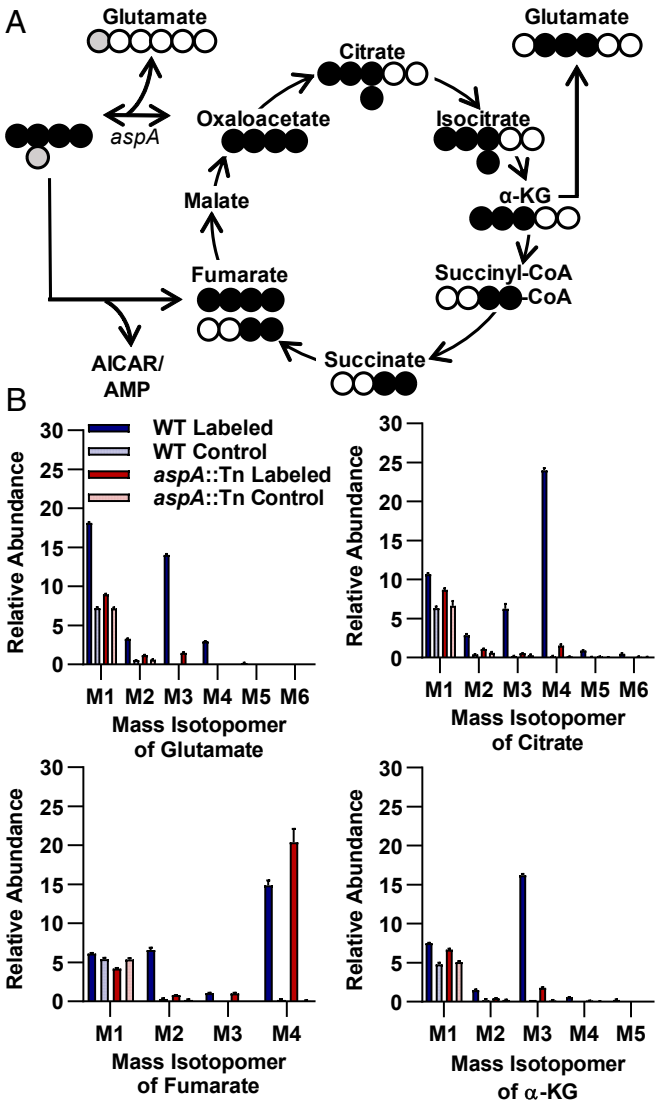

Fig. 4. Exogenous aspartate is shuttled into purine biosynthesis in an *aspA* mutant. (*A*) Schematic of carbon and nitrogen labeling following the addition of a [$^{13}C_4$,^{15}N]Asp tracer in a single round of TCA-cycle activity. Gray circles indicate heavy isotope-labeled nitrogen. Black circles indicate heavy isotope-labeled carbon. Open circles indicate unlabeled atoms. AICAR, amino-4-imidazolecarboxamide ribonucleotide 5′-phosphate. (*B*) Percent abundances of mass isotopomers relative to total metabolite abundance for select metabolites of WT or *aspA*::Tn mutant *S. aureus* grown in CDMG with [$^{13}C_4$,^{15}N]Asp or unlabeled Asp control for 2 h; $n = 3$ biologic replicates. Columns indicate the mean. Error bars represent SEM.

GltT Is a Functional Aspartate Transporter in *S. aureus*. An *aspA* mutant could only survive in vitro in CDMG when exogenous Asp is supplied, suggesting that *S. aureus* encodes a functional Asp transporter (Fig. 3 and *SI Appendix*, Fig. S6*A*). However, we found that an *aspA* mutant was unable to acquire sufficient Asp from bone for growth in vitro, suggesting that Asp levels within bone may be too low to support growth or that Asp transport is not functional (Fig. 3 and *SI Appendix*, Fig. S6*A*). This was surprising, as the concentration of all other amino acids within homogenized bone was sufficient to support the enhanced growth of WT *S. aureus* in amino acid-depleted media. Interestingly, Asp biosynthesis is also conditionally essential for growth in vitro in *Bacillus subtilis*, despite the ability to acquire Asp exogenously through the Asp/Glu transporter GltT (18). We therefore hypothesized that Asp transport may occur through the *S. aureus* GltT homolog (*SAUSA300_2329*). To test this hypothesis, we first examined the ability of *S. aureus* GltT to transport Asp. To confirm that GltT is the only functional transporter of Asp under our growth conditions, we generated an *aspA/gltT* double mutant. Although an *aspA* mutant was able to acquire exogenous Asp from CDMG, the *aspA/gltT* double mutant was incapable of growing in CDMG, suggesting that GltT is the only transporter for exogenous Asp under these conditions (Fig. 5*A* and *SI Appendix*, Fig. S6*B*). To further verify that GltT is the only Asp transporter functional under these conditions, we examined uptake of [$^{13}C_4$,^{15}N]Asp by GCMS (Fig. 5*B* and Dataset S2). In an *aspA/gltT* mutant background constitutively expressing *gltT* in trans on an overexpression construct driven by the constitutively active *lgt* promoter, Asp was readily taken up and converted into downstream intermediates, namely fumarate. However, in an *aspA/gltT* mutant background expressing an empty vector control, uptake of [$^{13}C_4$,^{15}N]Asp was not detected above background. Because *S. aureus* GltT is a homolog to an Asp/Glu transporter, the in vitro growth defect of an *aspA/gltT* mutant could be caused by a defect in Glu uptake. However, the primary Glu transporter in *S. aureus* was recently established as GltS (19). Furthermore, the requirement for GltT in an *aspA* mutant could be bypassed by supplying 2 mM asparagine (Asn), which is acquired through alternative transporters and converted to Asp by asparaginase (AnsA) (Fig. 5*A* and *SI Appendix*, Figs. S6*B* and S7) (20, 21). Therefore, the ability of Asn supplementation to bypass the growth defect of an *aspA/gltT* mutant indicates that the defect is not due to an inability to transport Glu but rather due to an inability to acquire Asp.

Excess Glutamate Competitively Inhibits *S. aureus* Aspartate Transport. *B. subtilis* requires Asp synthesis because Glu competitively inhibits Asp import through GltT, despite sufficiently high levels of Asp in media (18). Similar to *B. subtilis*, Asp transport in *S. aureus* is also competitively inhibited by Glu in vitro (20). We hypothesized that *S. aureus* Asp transport may be similarly inhibited by Glu in vivo and that the ratio of Glu to Asp in bone may prevent acquisition of exogenous Asp in vivo and in our ex vivo assay (20). To test the hypothesis that Glu is elevated relative to Asp in bone, we measured Asp and Glu levels in homogenized murine femurs. We found that Glu was approximately twofold higher than Asp in uninfected tissues and that Glu increased in infected tissues to approximately fourfold higher than Asp concentrations (Fig. 5*C*). We hypothesized that this ratio of Glu to Asp may inhibit acquisition of Asp by an *aspA* mutant. To test this hypothesis, we grew an *aspA* mutant in CDMG containing ratios of Glu and Asp that are found in healthy and infected bone and examined if Glu inhibits utilization of Asp in *S. aureus* in these conditions. We found that in CDMG containing the ratios of Asp and Glu in healthy bone (1:2) or in CDMG containing ratios of Asp and Glu found in

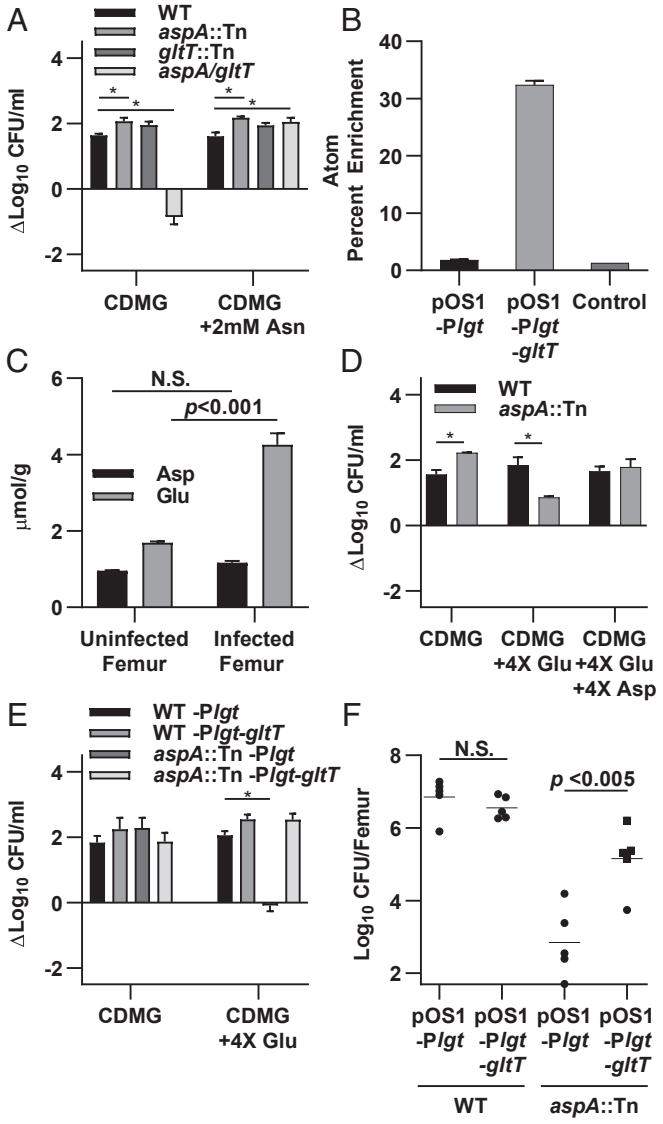

Fig. 5. GltT is an *S. aureus* aspartate transporter that is inhibited by excess glutamate in vitro. (*A*) The indicated strains were grown for 8 h in CDMG or CDMG supplemented with 2 mM Asn. (*B*) Atom percent enrichment of Asp for *aspA/gltT* expressing the indicated plasmids grown in CDMG with chloramphenicol (CM), 2 mM Asn, and [$^{13}C_4$,^{15}N]Asp or unlabeled Asp as a control for 2 h. (*C*) Asp and Glu concentrations were measured in uninfected and infected femurs 14 d postinfection. Glu-to-Asp ratio is 1.77 and 3.65 in uninfected and infected femurs, respectively. (*D*) WT or *aspA*::Tn *S. aureus* were grown in CDMG supplemented with 4× excess Glu or Asp and compared with growth in standard CDMG for 8 h. (*E*) The indicated strains were grown for 24 h in CDMG supplemented with excess Glu and CM compared with growth in standard CDMG and CM. Growth was monitored for 24 h due to enhanced lag phase induced by CM. (*F*) OM was induced in groups of mice using WT or *aspA*::Tn strains containing the indicated plasmids. Based on kinetic studies showing clearance of *aspA*::Tn between 1 and 7 d postinfection, femurs were processed for CFU enumeration at 4 d postinfection. Columns and horizontal bars indicate the mean. Error bars represent SEM. (*A*–*C*) $n = 3$ biologic replicates. (*C* and *F*) Significance was determined by Student's *t* test. (*D* and *E*) $n = 2$ biologic replicates. (*A*, *D*, and *E*) Significance was determined by two-way ANOVA with Holm–Sidak correction for multiple comparisons. *$P < 0.05$. N.S., not significant.

infected bone (1:4), growth of an *aspA* mutant was inhibited compared with WT *S. aureus* (Fig. 5*D* and *SI Appendix*, Fig. S6 *C* and *D*). Furthermore, this inhibition could be overcome by equalizing the Asp:Glu ratio in the media or by supplementation of media with Asn.

We next hypothesized that the inhibition of Asp transport could be overcome by increasing the expression of *gltT*, which might decrease saturation of the GltT transporter. Supporting this hypothesis, overexpression of *gltT* in trans rescued the growth defect of an *aspA* mutant in vitro in CDMG with excess Glu (Fig. 5*E* and *SI Appendix*, Fig. S6*E*). Furthermore, although an *aspA* mutant experiences a severe survival defect during OM by 4 d postinfection in vivo, constitutive expression of *gltT* provided a significant growth advantage to an *aspA* mutant (Fig. 5*F* and *SI Appendix*, Fig. S3*A*). Together, these data suggest that although *S. aureus* is able to acquire exogenous Asp through the GltT transporter, the excess Glu in some host tissue niches inhibits Asp transport and necessitates Asp biosynthesis in vivo for the synthesis of purines. Overall, this study characterizes the metabolic pathways involved in invasive staphylococcal infection during OM and highlights how the host nutrient milieu drives biosynthetic pathways required for bacterial survival.

Discussion

The ability of *S. aureus* to infect a variety of host tissue types requires metabolic flexibility to acquire or produce nutrients in different environments. Yet, the metabolic requirements for staphylococcal growth during invasive infection have not been fully elucidated. Using a combination of monoinfections and ex vivo growth analyses, we performed a comprehensive analysis of the metabolic requirements for *S. aureus* during OM. We determined that Asp biosynthesis represents a key metabolic node for staphylococcal survival during infection. Finally, we demonstrated that the nutritional context of bone dictates the metabolic strategies used by *S. aureus*.

Previous in vitro studies have focused on the metabolic capabilities of *S. aureus* in the absence of glucose, as the centers of abscesses are predicted to be glucose-limited (21). Transcript and protein levels of gluconeogenic enzymes in *S. aureus* have also been found to be elevated during invasive infection, and in OM specifically (22, 23). Our studies, however, suggest that *S. aureus* requires glycolysis and glycolytic carbon sources to survive in vivo during OM. *S. aureus* is known to have a remarkable ability to scavenge glucose from its environment due to an arsenal of four high-affinity glucose transporters (24). This preference for glycolytic metabolism reflects the adaptation of *S. aureus* to nonrespiratory conditions within inflamed tissues (25). The conflicting increase of gluconeogenic enzymes previously observed with the requirement for glycolysis observed here may reflect temporal changes or spatial heterogeneity in glucose availability during infection.

The TCA cycle has been suggested to be important for staphylococcal virulence (26–28). When we tested mutants from each of the pathways involved in the TCA cycle individually, however, none of the TCA-cycle enzymes were required for survival during OM. The lack of a virulence defect in TCA-cycle mutants in our model is not surprising, as multiple factors present in bone during infection are known to reduce TCA-cycle activity/expression, including reactive oxygen/nitrogen species, iron limitation, and glycolytic carbon source availability (29–33). Interestingly, in WT *S. aureus*, [$^{13}C_4$,^{15}N]Asp was observed to contribute to TCA-cycle intermediates in the presence of glucose, suggesting that, despite catabolite repression of some TCA-cycle enzymes, some TCA-cycle activity still occurs in vitro, which may impact antibiotic tolerance (33). Despite potential low-level activity of the TCA cycle during growth on glucose in vitro, these results collectively demonstrate that the TCA cycle is not required for full bacterial burdens in bone.

We found that *S. aureus* requires biosynthesis of Asp for survival during OM and disseminated infection. This finding appears to be characteristic of invasive infection, as several other groups have identified *aspA* as essential for survival in unbiased screens in vivo (34, 35). Our data indicate that *S. aureus* depends

upon endogenous Asp biosynthesis despite the presence of exogenous Asp in bone. This is due, in part, to inhibition of Asp transport by higher concentrations of Glu in infected bone. Although we demonstrated that the Glu:Asp ratio of infected bone is increased compared with uninfected bone, we suspect that these levels are underestimated, as the spatial distribution of analytes is destroyed by traditional metabolite analysis. In fact, local tissue Glu levels have been found to increase more than 30-fold within staphylococcal brain abscesses (36). Glutamate levels may, therefore, be significantly higher surrounding the infection site.

The dependence of *S. aureus* on endogenous Asp synthesis may reflect the specificity of GltT for both Asp and Glu. The inability of an *aspA* mutant to survive in host tissues has previously been attributed to the low level of Asp and Asn found in sera (37). Although Asn does appear to be limiting in bone, our observations suggest that the capacity of *S. aureus* to utilize exogenous amino acids, particularly Asp, is dependent not only on total amino acid levels and transporter presence but also on the context of the nutrient milieu and transporter functionality. Our results suggest that GltT is the only functional Asp transporter under the conditions tested, though it is possible that other Asp transporters are repressed or inactive. *S. aureus* may have therefore adapted to rely on Asp biosynthesis to overcome Asp transport limitations through the conserved GltT transporter.

The phenotype of an *aspA* mutant appears to be largely driven by an inability to synthesize purines in the absence of Asp. Inhibition of the purine synthesis pathway is known to cause defects in pathogenesis for a variety of bacterial pathogens, and several high-throughput screens have identified purine synthesis genes in *S. aureus* as required for bacterial growth and survival in mammalian tissues (34, 38–40). Furthermore, defects in Asp availability have been linked to insufficient purine biosynthesis in humans as well (41). *S. aureus* has also been shown to rely on synthesis of adenosine and deoxyadenosine for intoxication of the purine salvage pathway in phagocytes in vivo, suggesting that *S. aureus* may have an enhanced need for de novo purine biosynthesis to support virulence in vivo, beyond simple metabolic requirements (42, 43). Our results provide a potential explanation for the survival defect of *S. aureus* Asp biosynthesis mutants in vivo.

Although our study represents an in-depth examination of the metabolic pathways required for *S. aureus* survival in vivo during OM, these analyses do not account for the substantial temporal and spatial differences in bacterial metabolism that may occur during infection (44). Nutrient availability can vary widely within a single infection site and between tissues, necessitating additional studies to comprehensively characterize metabolite heterogeneity in vivo. However, overall, our studies define the nutritional capabilities of a unique infection site, bone, to support the growth of an invasive pathogen in vivo. These data emphasize the importance of characterizing the nutritional milieu within the host tissue environment for establishing a comprehensive understanding of the metabolic needs of pathogens during infection.

Materials and Methods

Bacterial Strains and Culture Conditions. Strain LAC (AH1263) served as the WT background unless otherwise stated (45). Transposon mutants were created by phi-85–mediated transduction of disrupted alleles from the respective mutants obtained from the NARSA transposon library (46). Strain Δ*pyk*::erm in the LAC background was created by bacteriophage phi-85–mediated transduction of Δ*pyk*::erm in the Newman background (25). WT Newman background and strain Δ*pfkA* were previously described (47). Plasmids and complementation constructs were created as previously described (48, 49) (*SI Appendix*).

Murine Models of Infection. All experiments involving animals were reviewed and approved by the Institutional Animal Care and Use Committee at Vanderbilt University Medical Center. All experiments were performed according to NIH guidelines, the Animal Welfare Act, and US Federal law. OM was induced in 7- to 8-wk-old female C57BL/6J mice using an inoculum of ∼1×10^6 colony-forming units (CFUs) delivered into murine femurs as previously reported (7). Disseminated *S. aureus* infection was induced in 7-wk-old female C57BL/6J mice by retroorbital inoculation of ∼5×10^7 CFUs. At various times postinfection, mice were killed, and the infected tissue was processed for CFU enumeration by homogenization and subsequent plating at limiting dilution on tryptic soy agar (TSA). Limit of detection is 49 CFUs per femur, heart, and both kidneys combined, and 99 CFUs per liver.

Comparative Growth Analysis and Chemically Defined Medium Composition. Chemically defined media with glucose were prepared as previously described (50) (*SI Appendix*). For comparative growth analysis, overnight cultures of WT and mutant strains were washed in phosphate-buffered saline (PBS) and backdiluted 1:1,000 into CDMG and grown in 96-well plates at 37 °C with orbital shaking at 180 rpm. Viable CFUs were measured by plating on TSA at the time points indicated. Growth is reported as $\Delta \log_{10}$ CFU/mL compared with inocula at 0 h. To make CDMG supplemented with homogenized bone, femurs from 8- to 11-wk-old female C57BL/6J mice were harvested and frozen at −80 °C prior to use. Immediately prior to inoculating media with bacteria, femurs were homogenized in 500 μL of CelLytic MT Cell Lysis Reagent (Sigma) and added at 5% vol/vol (V/V), which was experimentally determined to give optimal WT *S. aureus* growth in vitro. As an internal control, equivalent volumes of cell lysis reagent were added to CDMG as needed.

Enzymatic Determination of Metabolite Levels. Femurs were harvested from 8-wk-old female C57BL/6J mice and frozen immediately on dry ice. Tissues were stored at −80 °C before being homogenized in 500 μL of PBS. Asp and Glu concentrations were measured by the Aspartate Colorimetric Assay Kit (BioVision) and EnzyChrom Glutamate Assay Kit (BioAssay Systems), respectively, according to manufacturer instructions. Absorbances were measured by a BioTek Synergy HT 96-well plate reader. Metabolite concentrations were normalized to wet tissue weight.

[^{13}C,^{15}N]Aspartate Tracer Studies. *S. aureus* was grown overnight in tryptic soy broth (TSB) with antibiotics as needed. Cultures were then washed and backdiluted 1:100 in CDMG or CDMG with 2 mM Asn as indicated. Cultures were grown for 2 h before pelleting and resuspending in fresh media containing [$^{13}C_4$,^{15}N]Asp at equivalent molarity as standard CDMG. Cultures were allowed to grow in [$^{13}C_4$,^{15}N]Asp-containing media for up to 2 h before rapidly chilling with an equal ratio of ice-cold PBS. Cultures were washed in PBS a total of three times before pelleting and processing for GCMS as previously described (51), with the following modification: Metabolites were converted to methoxime *tert*-butyldimethylsilyl derivatives by reaction with 70 μL *N*-tertbutyldimethylsilyl-*N*-methyltrifluoroacetamide (MTBSTFA) + 1% tert-butyldimethylchlorosilane (TBDMCS) (Regis Technologies).

Graphical and Statistical Analysis. Statistical analyses were performed using Prism 7.0 (GraphPad Software).

Data Availability. Additional methods and other relevant data are in Datasets S1 and S2 and *SI Appendix*. The data supporting the findings of this study are available within the article and its supplementary materials.

ACKNOWLEDGMENTS. J.E.C. was supported by NIH Grants R01AI132560, R01AI145992, and K08AI113107 and a Career Award for Medical Scientists from the Burroughs Wellcome Fund. A.D.P. was supported by NIH Grants T32AI11254 and F31AI133970. C.A.F. was supported through NIH Grant T32GM007347 and is supported by NIH Grant F30AI138424. C.E.B. is supported by NIH Grant T32AI11254. J.D.Y. is supported by NIH Grants R01DK106348 and U01CA235508.

1. M. J. Kuehnert *et al*., Prevalence of *Staphylococcus aureus* nasal colonization in the United States, 2001-2002. *J. Infect. Dis.* **193**, 172–179 (2006).
2. A. R. Richardson, G. A. Somerville, A. L. Sonenshein, Regulating the intersection of metabolism and pathogenesis in gram-positive bacteria. *Microbiol. Spectr.* **3**, MBP-0004-2014 (2015).
3. G. A. Somerville, R. A. Proctor, At the crossroads of bacterial metabolism and virulence factor synthesis in Staphylococci. *Microbiol. Mol. Biol. Rev.* **73**, 233–248 (2009).
4. J. S. Gerber, S. E. Coffin, S. A. Smathers, T. E. Zaoutis, Trends in the incidence of methicillin-resistant *Staphylococcus aureus* infection in children's hospitals in the United States. *Clin. Infect. Dis.* **49**, 65–71 (2009).
5. D. P. Lew, F. A. Waldvogel, Osteomyelitis. *Lancet* **364**, 369–379 (2004).
6. T. Liu, X. Zhang, Z. Li, D. Peng, Management of combined bone defect and limb-length discrepancy after tibial chronic osteomyelitis. *Orthopedics* **34**, e363–e367 (2011).

7. J. E. Cassat *et al*., A secreted bacterial protease tailors the *Staphylococcus aureus* virulence repertoire to modulate bone remodeling during osteomyelitis. *Cell Host Microbe* **13**, 759–772 (2013).
8. N. E. Putnam *et al*., MyD88 and IL-1R signaling drive antibacterial immunity and osteoclast-driven bone loss during *Staphylococcus aureus* osteomyelitis. *PLoS Pathog.* **15**, e1007744 (2019).
9. E. Esen, F. Long, Aerobic glycolysis in osteoblasts. *Curr. Osteoporos. Rep.* **12**, 433–438 (2014).
10. J. M. Kim *et al*., Osteoclast precursors display dynamic metabolic shifts toward accelerated glucose metabolism at an early stage of RANKL-stimulated osteoclast differentiation. *Cell. Physiol. Biochem.* **20**, 935–946 (2007).
11. W. A. Peck, S. J. Birge Jr., S. A. Fedak, Bone cells: Biochemical and biological studies after enzymatic isolation. *Science* **146**, 1476–1477 (1964).
12. D. V. Cohn, B. K. Forscher, Aerobic metabolism of glucose by bone. *J. Biol. Chem.* **237**, 615–618 (1962).
13. A. D. Wilde *et al*., Bacterial hypoxic responses revealed as critical determinants of the host-pathogen outcome by TnSeq analysis of *Staphylococcus aureus* invasive infection. *PLoS Pathog.* **11**, e1005341 (2015).
14. N. D. Hammer *et al*., Inter- and intraspecies metabolite exchange promotes virulence of antibiotic-resistant *Staphylococcus aureus*. *Cell Host Microbe* **16**, 531–537 (2014).
15. C. J. Alteri, S. D. Himpsl, H. L. Mobley, Preferential use of central metabolism in vivo reveals a nutritional basis for polymicrobial infection. *PLoS Pathog.* **11**, e1004601 (2015).
16. E. Bosi *et al*., Comparative genome-scale modelling of *Staphylococcus aureus* strains identifies strain-specific metabolic capabilities linked to pathogenicity. *Proc. Natl. Acad. Sci. U.S.A.* **113**, E3801–E3809 (2016).
17. Y. Oogai *et al*., Lysine and threonine biosynthesis from aspartate contributes to *Staphylococcus aureus* growth in calf serum. *Appl. Environ. Microbiol.* **82**, 6150–6157 (2016).
18. H. Zhao, D. M. Roistacher, J. D. Helmann, Aspartate deficiency limits peptidoglycan synthesis and sensitizes cells to antibiotics targeting cell wall synthesis in *Bacillus subtilis*. *Mol. Microbiol.* **109**, 826–844 (2018).
19. M. S. Zeden, I. Kviatkovski, V. T. Chittezham, P. D. Fey, A. Gründling, *Staphylococcus aureus* can survive in the absence of c-di-AMP upon inactivation of the main glutamine transporter. bioRxiv:10.1101/754309 (1 September 2019).
20. S. A. Short, D. C. White, H. R. Kaback, Mechanisms of active transport in isolated bacterial membrane vesicles. IX. The kinetics and specificity of amino acid transport in *Staphylococcus aureus* membrane vesicles. *J. Biol. Chem.* **247**, 7452–7458 (1972).
21. C. R. Halsey *et al*., Amino acid catabolism in *Staphylococcus aureus* and the function of carbon catabolite repression. *MBio* **8**, e01434-16 (2017).
22. D. J. Ryan *et al*., MicroLESA: Integrating autofluorescence microscopy, in situ microdigestions, and liquid extraction surface analysis for high spatial resolution targeted proteomic studies. *Anal. Chem.* **91**, 7578–7585 (2019).
23. A. K. Szafranska *et al*., High-resolution transcriptomic analysis of the adaptive response of *Staphylococcus aureus* during acute and chronic phases of osteomyelitis. *MBio* **5**, e01775-14 (2014).
24. N. P. Vitko, M. R. Grosser, D. Khatri, T. R. Lance, A. R. Richardson, Expanded glucose import capability affords *Staphylococcus aureus* optimized glycolytic flux during infection. *MBio* **7**, e00296-16 (2016).
25. N. P. Vitko, N. A. Spahich, A. R. Richardson, Glycolytic dependency of high-level nitric oxide resistance and virulence in *Staphylococcus aureus*. *MBio* **6**, e00045-15 (2015).
26. G. A. Somerville *et al*., *Staphylococcus aureus* aconitase inactivation unexpectedly inhibits post-exponential-phase growth and enhances stationary-phase survival. *Infect. Immun.* **70**, 6373–6382 (2002).
27. G. A. Somerville *et al*., Synthesis and deformylation of *Staphylococcus aureus* delta-toxin are linked to tricarboxylic acid cycle activity. *J. Bacteriol.* **185**, 6686–6694 (2003).
28. B. Dassy, J. M. Fournier, Respiratory activity is essential for post-exponential-phase production of type 5 capsular polysaccharide by *Staphylococcus aureus*. *Infect. Immun.* **64**, 2408–2414 (1996).
29. K. Seidl *et al*., *Staphylococcus aureus* CcpA affects biofilm formation. *Infect. Immun.* **76**, 2044–2050 (2008).
30. K. Seidl *et al*., Effect of a glucose impulse on the CcpA regulon in *Staphylococcus aureus*. *BMC Microbiol.* **9**, 95 (2009).
31. U. E. Schaible, S. H. Kaufmann, Iron and microbial infection. *Nat. Rev. Microbiol.* **2**, 946–953 (2004).
32. D. B. Friedman *et al*., *Staphylococcus aureus* redirects central metabolism to increase iron availability. *PLoS Pathog.* **2**, e87 (2006).
33. S. E. Rowe *et al*., Reactive oxygen species induce antibiotic tolerance during systemic *Staphylococcus aureus* infection. *Nat. Microbiol.* **5**, 282–290 (2020).
34. M. D. Valentino *et al*., Genes contributing to *Staphylococcus aureus* fitness in abscess- and infection-related ecologies. *MBio* **5**, e01729-14 (2014).
35. M. R. Grosser *et al*., Genetic requirements for *Staphylococcus aureus* nitric oxide resistance and virulence. *PLoS Pathog.* **14**, e1006907 (2018).
36. B. Hassel *et al*., Brain infection with *Staphylococcus aureus* leads to high extracellular levels of glutamate, aspartate, γ-aminobutyric acid, and zinc. *J. Neurosci. Res.* **92**, 1792–1800 (2014).
37. B. M. Benton *et al*., Large-scale identification of genes required for full virulence of *Staphylococcus aureus*. *J. Bacteriol.* **186**, 8478–8489 (2004).
38. E. M. Kofoed *et al*., De novo guanine biosynthesis but not the riboswitch-regulated purine salvage pathway is required for *Staphylococcus aureus* infection in vivo. *J. Bacteriol.* **198**, 2001–2015 (2016).
39. S. Samant *et al*., Nucleotide biosynthesis is critical for growth of bacteria in human blood. *PLoS Pathog.* **4**, e37 (2008).
40. J. Connolly *et al*., Identification of *Staphylococcus aureus* factors required for pathogenicity and growth in human blood. *Infect. Immun.* **85**, e00337-17 (2017).
41. L. B. Sullivan *et al*., Supporting aspartate biosynthesis is an essential function of respiration in proliferating cells. *Cell* **162**, 552–563 (2015).
42. V. Thammavongsa, J. W. Kern, D. M. Missiakas, O. Schneewind, *Staphylococcus aureus* synthesizes adenosine to escape host immune responses. *J. Exp. Med.* **206**, 2417–2427 (2009).
43. V. Winstel, D. Missiakas, O. Schneewind, *Staphylococcus aureus* targets the purine salvage pathway to kill phagocytes. *Proc. Natl. Acad. Sci. U.S.A.* **115**, 6846–6851 (2018).
44. J. E. Cassat *et al*., Integrated molecular imaging reveals tissue heterogeneity driving host-pathogen interactions. *Sci. Transl. Med.* **10**, eaan6361 (2018).
45. B. R. Boles, M. Thoendel, A. J. Roth, A. R. Horswill, Identification of genes involved in polysaccharide-independent *Staphylococcus aureus* biofilm formation. *PLoS One* **5**, e10146 (2010).
46. P. D. Fey *et al*., A genetic resource for rapid and comprehensive phenotype screening of nonessential *Staphylococcus aureus* genes. *MBio* **4**, e00537-12 (2013).
47. L. A. Mike *et al*., Activation of heme biosynthesis by a small molecule that is toxic to fermenting *Staphylococcus aureus*. *Proc. Natl. Acad. Sci. U.S.A.* **110**, 8206–8211 (2013).
48. J. Chen, P. Yoong, G. Ram, V. J. Torres, R. P. Novick, Single-copy vectors for integration at the SaPI1 attachment site for *Staphylococcus aureus*. *Plasmid* **76**, 1–7 (2014).
49. J. Bubeck Wardenburg, W. A. Williams, D. Missiakas, Host defenses against *Staphylococcus aureus* infection require recognition of bacterial lipoproteins. *Proc. Natl. Acad. Sci. U.S.A.* **103**, 13831–13836 (2006).
50. N. P. Vitko, A. R. Richardson, Laboratory maintenance of methicillin-resistant *Staphylococcus aureus* (MRSA). *Curr. Protoc. Microbiol.*, chap. 9, unit 9C.2 (2013).
51. L. J. Jazmin *et al*., Isotopically nonstationary ^{13}C flux analysis of cyanobacterial isobutyraldehyde production. *Metab. Eng.* **42**, 9–18 (2017).